Demonstration of a cryocooled 10 GHz oscillator with 10^{-15} frequency stability.

S. Grop [1], P.Y. Bourgeois [1], N. Bazin [1], Y. Kersalé [1], E. Rubiola [1], C. Langham[2], M. Oxborrow [2], D. Clapton[3], S. Walker[3], J. De Vicente [4], V. Giordano [1]

[1]: FEMTO–ST Institute,
Time and Frequency Dpt., UMR 6174 CNRS-ENSMM
32 av. de l'Observatoire, 25044 Besançon Cedex, France
[2]: National Physical Laboratory
Queens Road
Teddington, Middlesex, TW11 0LW, UK
[3]: Oxford Instruments plc
Tubney Woods
Abingdon, Oxon OX13 5QX, UK
[4]: European Space Agency ESA-ESOC
Robert Bosch Str. 5
D-64293 Darmstadt, Germany

1 Abstract

This paper reports the breadboarding and the validation of a 10 GHz ultra-stable Cryogenic Sapphire Oscillator (CSO) operated in an autonomous cryocooler. This CSO presents a frequency stability better than 3×10^{-15} between 1 s and 1,000 s and a phase noise lower than -100 dBc/Hz at 1 Hz.

2 Introduction

The ever increasing need for better tracking data and scientific return in deep space missions calls for the development of new frequency references of improved stability. Ground stations of the European Space Agency (ESA) are conventionnaly equipped with hydrogen masers (HM) which are the most stable commercial atomic clocks around 1000 s – 1 day timescales ($\sigma_y(\tau \approx 1000\text{s}) < 10^{-15}$).

The Elisa project founded by the ESA has as main objective the demaonstration of a 3×10^{-15} short term frequency stability associated with a large autonomy of one year and more. This project was realized in collaboration between FEMTO-ST Institute, the NPL and the Timetech Gmbh company.

Cryogenic Sapphire Oscillators (CSO) offer unbeatable stability performances in timescales ranging from milliseconds to a few hundred seconds, and therefore extremely low phase noise close to the carrier. A combined CSO and HM system in ESA deep space stations would allow to benefit from excellent short term and long stabilities. Compared to the current performances available from hydrogen masers and state of the art quartz oscillators, CSO would provide the means to improve the orbit determination and would open the field to new radio science experiments.

3 ELISA sub-systems

The scheme in figure 1 describes the main sub-systems constituting the Elisa frequency reference.

The heart of the system is a whispering gallery mode sapphire resonator made of a large and thick high purity sapphire crystal (HEMEX grade [1]) cylinder placed in the center of a copper cavity (see section 4). This assembly is thermally connected to the second stage of a pulse tube cryocooler. A special "soft" thermal link and a thermal ballast (see section 5) were designed in order to filter the vibrations and the temperature modulation at about 1 Hz induced by the gas flow in the cryocooler.

Low thermal conductance coaxial cables are used to connect the Sapphire resonator to the sustaining loop placed at room temperature. The oscillating circuit is completed by two servos stabilizing the phase along the loop and the power injected into the resonator. These control loops use the same principle as those described in the reference [12] (see section 6). Apart from the CSO signal at a frequency ν_0, we have to generate three other frequencies required for ESA

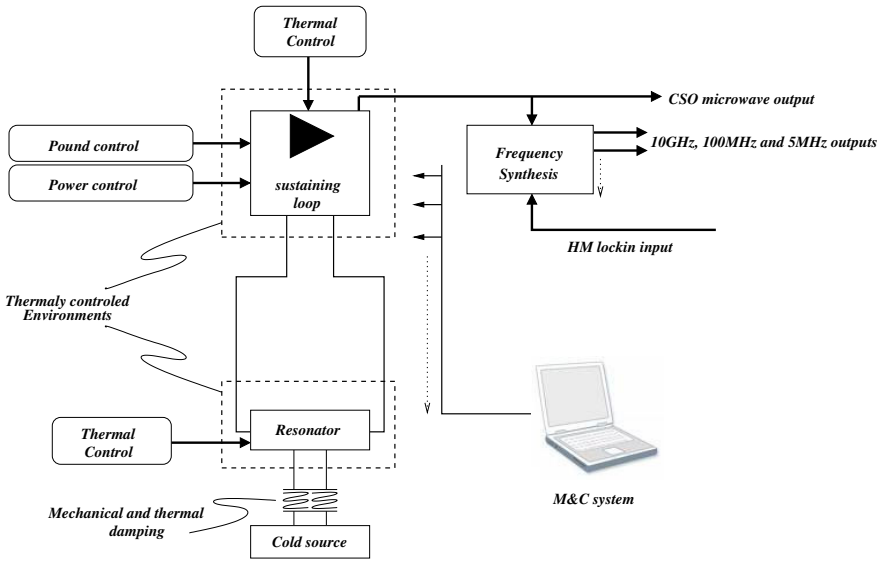

Figure 1: ELISA sub-systems. The frequency reference is a sapphire resonator maintained at a low temperature (≈ 6K) in a closed cycle cryocooler. The CSO delivers a signal at the frequency ν_0 which serves as reference for a frequency synthesis subsystem delivering the useful frequencies

applications: 10 GHz, 100 MHz and 5 MHz. Moreover these useful signals should be phase locked at long term on a 100 MHz reference coming from a Hydrogen Maser (HM). A frequency synthesis was then designed to transfer the CSO's frequency stability to these useful signals with a slight degradation at 5 MHz as a result of the performance of typical RF components.

4 Sapphire resonator

The frequency reference is a cylindrical sapphire resonator in which high order modes called whispering gallery (WG) modes can be excited. These modes are characterized by a high energy confinement in the dielectric due to the total reflexion at the vacuum-dielectric interface. As sapphire shows the lowest dielectric losses in the microwave range, a Q-factor as high as 1 billion can be obtained at the liquid-He temperature.

The pure sapphire resonator does not have the frequency-vs-temperature turning point otherwise found in most piezoelectric resonators after appropriate design. Although the mode frequency thermal sensitivity decreases significantly at low temperature, it never goes low enough for the target stability to be achieved with state-of-the-art temperature control. Fortunately, it turns out that high-purity sapphire crystals always contain a small concentration of paramagnetic impurities, such as Cr^{3+}, Fe^{3+} or Mo^{3+}. These ions induce a small magnetic permeability whose temperature dependence compensates at a given temperature T_0 for the natural sapphire resonator thermal sensitivity. This turnover temperature T_0 depends on the mode and on the impurity concentration but for many of the resonators tested by different groups, the turnover temperature is generally in the range $5 - 8$K. This thermal compensation relaxes dramatically the thermal stabilization requirements. Indeed, with such a thermal compensation phenomena, the frequency stability objective of 3×10^{-15} can be obtained with a ± 1 mK thermal stabilization which can be easily fulfilled with commercial cryogenic temperature controllers.

The resonator size and WG mode order determine the resonant frequency and the unloaded Q-factor. Experience shows that the best results are obtained with a resonator presenting a ratio diameter over height of the order of $D/H \approx 3/5$ [11] and with WG modes between 13 and 18. The energy confinement in the dielectric improves as the mode order increases. This fact has two practical consequences: 1) Q is progressively degraded at lower-order modes (less than 13) because of electromagnetic radiation, and 2) high order modes (greater than 18) are difficult or impossible to exploit because the couplers need too sharp adjustment. Another difficulty connected with high-order modes is the presence of many spurious modes, which makes the frequency selection difficult. For practical reasons the resonator size can not be too large. A resonator diameter D of about 50 mm is comfortable for mechanics and cryogenics. This means that the resonant frequency should not be lower than 9 GHz. Dielectric dissipation in sapphire increases as frequency increases.

This phenomenon sets a soft upper limit at some 13 GHz. This limit is about independent of the resonator size. Finally, the resonance of the Cr^{3+} ion at 11.45 GHz, and the resonance of the Fe^{3+} ion and 12.04 GHz are to be avoided. A margin of ± 200 MHz is recommended. Figure 2 summarizes the frequency selection rules we adopted. This figure represents the relation between the resonator diameter and its resonance frequency for the WGH mode family assuming $D/H = 3/5$.

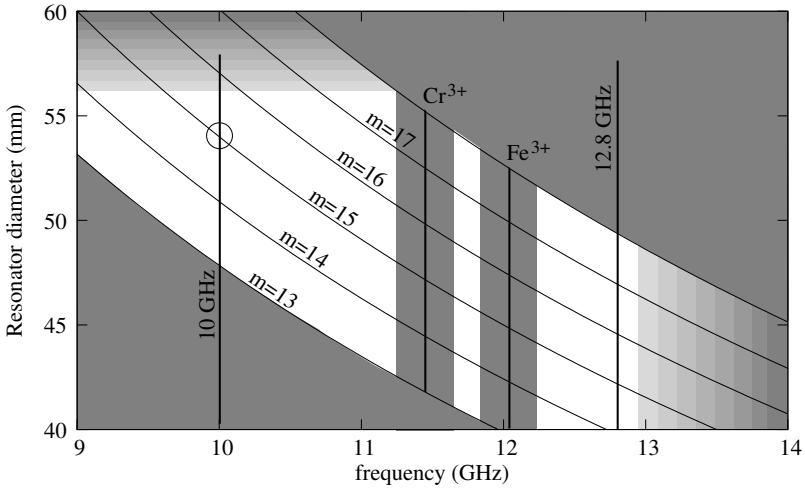

Figure 2: *Resonator frequency selection rules. The chosen resonator parameters correspond to the point highlighted by the circle: frequency* $\nu_0 = 10$ *GHz, diameter* $D \approx 54$*mm, azimuthal number* $m = 15$

4.1 Design approach

The design strategy was to define a "round" resonant frequency to simplify the development of the frequency synthesis.

After refining the electromagnetic model [10], we are able to design a resonator with a high-Q mode at the frequency ν_0 of our choice. The electrical and mechanical tolerances yield a frequency accuracy of $5{\times}10^{-4}$ (± 5 MHz at 10 GHz) and a reproducibility of 10^{-4} (± 1 MHz at 10 GHz). That said, we chose a resonant frequency $\nu_0 = \nu_{00} - \delta_{RF}$, where ν_{00} is a comfortable round value, and $\delta_{RF} = 10 \pm 5$ MHz. This choice is justified by the fact that a single-chip direct digital synthesizer (DDS) has the desired resolution and provides sufficient stability and spectral purity if the output frequency does not exceed some 15–20 MHz. Additionally, δ_{RF} cannot be too low frequency (< 5 MHz), otherwise it is difficult to avoid the spur of frequency ν_0, too close to ν_{00}. In this conditions, a DDS fits the needs for the correction δ_{RF} The nominal size of the resonator makes $\nu_0 < \nu_{00}$, so the correction $-\delta_{RF}$ takes a negative value. It is still possible to thin the resonator so that $\nu_0 = \nu_{00} + \delta_{RF}$, which can fix a number of mistakes without modifying the electronics.

Figure 2 suggests that ν_{00} can be either 10 GHz or 12.8 GHz, so that a low-noise 100 MHz output can be obtained from a cascade of by-10 or power-of-2 commercial frequency dividers. The value $\nu_{00} = 10$ GHz has been chosen because low-flicker SiGe amplifiers [2, 13] are available at this frequency, while 12.8 GHz falls beyond a sharp cutoff.

Our design strategy has three additional merits connected to the low value of the interpolation frequency δ_{RF}. The first one is that it simplifies the synthesizer. The second one is that the synthesizer can be over-engineered for high stability and low noise at a reasonably low cost. If a lucky oscillator exceeds the expected stability, the benefit is not lost. The third one is that the synthesizer can be tested without the oscillator, which simplifies the logistics and speeds up the validation process.

4.2 Resonator realization and validation

By using a Finite Elements analysis, we get a $WGH_{15,0,0}$ mode at 9.99 GHz with $D = 54.2$ mm and $H = 30$ mm. Taking into account the machining possibilities and the cost, we eventually ordered two sapphire pieces with $D = 54.2\text{mm} \pm 10\mu\text{m}$ and $H = 30\text{mm} \pm 20\mu\text{m}$. The resonator frequency is then defined as 9.99 GHz ± 3.5 MHz.
The resonator has a spindle (diameter 10 mm, length 22 mm) to be clamped from below. Such a mounting enables to reduce the mechanical stress on the region where the electromagnetic field is confined [5]. Two quasi identical resonators were machined from the same HEMEX sapphire boule by the Crystal System company. One of the two resonators named

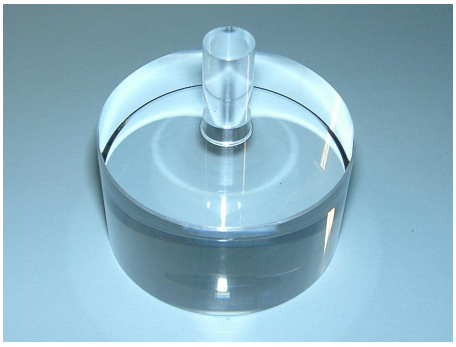

Figure 3: *HEMEX high grade sapphire resonator.*

Elisa and Alizée are shown on the figure 3.

The resonator is clamped on the inferior plate closing the gold plated copper cavity. The latter is maintained in thermal contact with the cooling source through a copper piece in which a thermal sensor and a heater are anchored. To couple the resonator to the external circuit, we use two small magnetic loops intercepting the H_φ magnetic field component of the resonator.

Table 1 summarizes the main characteristics of the two resonators at their turnover temperature T_0. The adjustment of the coupling coefficients have been obtained after few cool-downs.

Table 1: Resonators parameters

	ν_0 (GHz)	T_0 (K)	Q_L	β_1	β_2	IL (dB)
ELISA	$9.989,121$	6.13	7.4×10^8	1	≈ 0.02	-24.9
ALIZEE	$9.988,370$	6.05	6.9×10^8	1.09	≈ 0.02	-26

5 CRYOCOOLER

The key point that made us opt for the cryocooler option is that unlike bath cryostat, they don't need regular refills of liquid helium. These refillings disturb the sapphire resonator which needs around two days to recover. Nevertheless two problems had to be solved: the vibrations level and the temperature fluctuations of the cryocooler cold stage. We measured temperature fluctuations of ± 100 mK on a Cryomech PT405 with a 1.3 Hz frequency corresponding to the gas cycle in the system.

Oxford Instruments supplied a 4K Cryofree® cryostat modified to achieve the performance required by the ELISA project. This cryocooler fulfilled of a low displacement on the experiment plate (less than two microns in three axes) with a temperature stabilization of ± 1 mK over 1000 s and a cooling power at 4K of 50 mW. The cryocooler used by Oxford Instruments is a two-stage pulse-tube refrigerator with a rotary valve decoupled from the main dewar, eliminating the need for moving parts in the cold head. The cryostat design of the vibration reduction system is similar to those described in the references [16, 4]. The Oxford Instruments design is represented in figure 4.

The two stages of the cryostat (70K shield and 4K cold plate) are thermally linked to the cryocooler stages with floppy copper heat links. The support thin-wall tubes are mounted like an hexapod to give rigidity to the system. To limit the temperature fluctuations of the cold stage, a gadolinium gallium garnet (GGG) crystal [6] was mounted between this stage and a copper temperature stabilization block supporting the experiment using four legs. The four legs provided a tuned weak thermal link to optimize the temperature stability and cooling power of the cryostat. Few combinations of materials for the legs were used and the optimized performance was obtained when using two stainless steel and two brass/copper legs.

A three axis accelerometer was fixed on the experimental plate and we measured less than 1 μm vibration in x, y and z direction [9]. The base temperature at stabilization stage with the customer wiring is 6K with 50 mW applied to the stabilization stage for a maximum of fluctuations of 1mK.

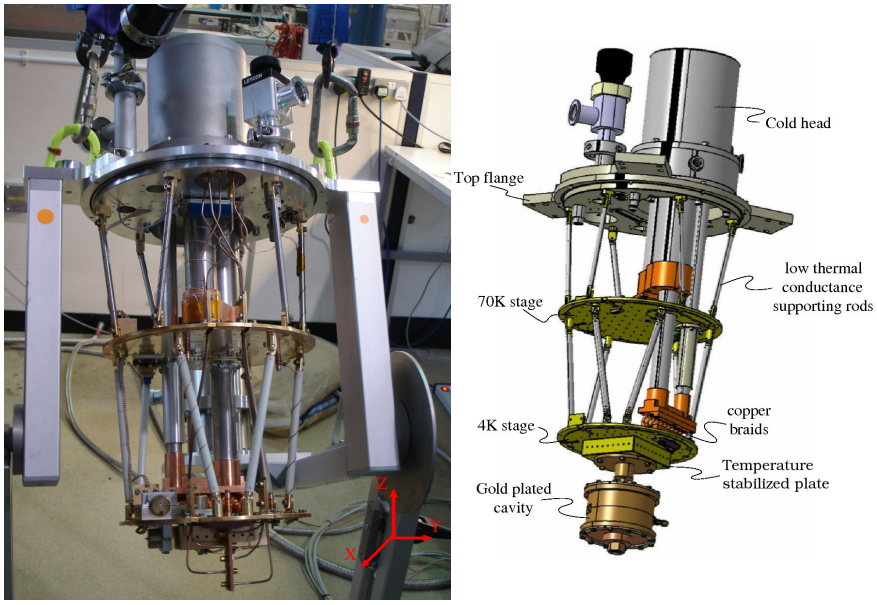

Figure 4: *Crycooler internal design.*

6 OSCILLATOR

The oscillator circuit is described in Fig. 5. It is a classical transmission oscillator circuit with two additional servo loops that control the phase and the power of the circulating signal. These two servos are mandatory to get a high frequency stability.

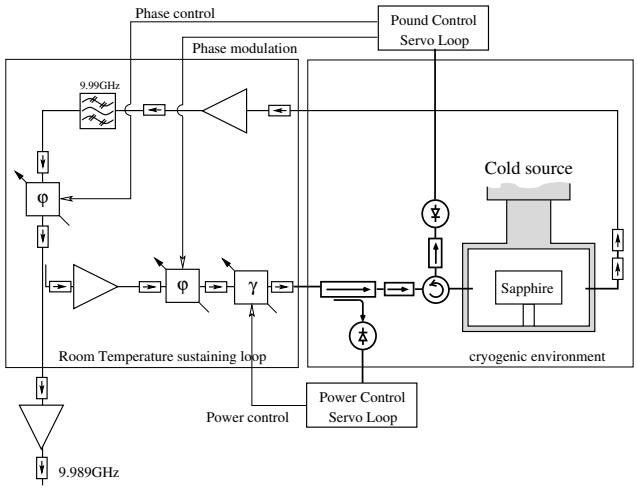

Figure 5: *Elisa oscillator design. The sustaining loop is completed with two additional servo loops stabilizing the phase of the circulating signal and the power injected inside the resonator.*

The first servo loop is based on the Pound frequency discriminator principle [7, 8, 3], it ensures that the CSO oscillates at the resonator frequency ν_0 by compensating any variation of the phase lag along the loop.

Due to the radiation pressure and to the self resonator heating, the resonator frequency presents a power sensitivity of the order of 4×10^{-11}/mW. The power servo loop ensures that the power injected into the resonator stays constant.

7 FREQUENCY SYNTHESIS

The frequency synthesis principle is given in Fig. 6. A Dielectric Resonator Oscillator is phase locked to the CSO. The frequency offset of the cryogenic oscillator is compensated with a low noise DDS. Commercial frequency dividers enable to reach the operational frequencies of 100MHz and 5MHz.

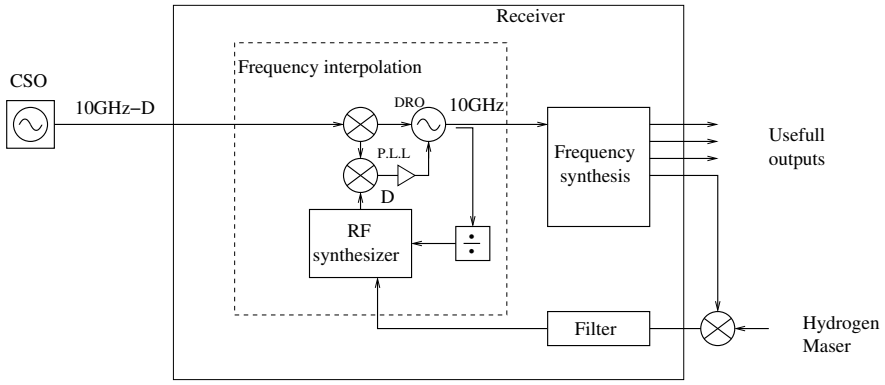

Figure 6: *Scheme of the frequency synthesis developed by Timetech Gmbh.*

8 PERFORMANCES

8.1 Frequency stability and phase noise measurement

To evaluate the relative frequency stability of Elisa, it has been compared with a second CSO build around the second resonator Alizée which is cooled in a liquid helium dewar. Apart from the cooling method, the two CSOs are quasi identical.

The time domain measurement technique is a standard one: the two oscillator signals are mixed to get a beatnote at the frequency difference which is of about 745 kHz. The beat signal is directly sent to a high resolution counter and the Allan deviation σ_y is computed from data averaged over 1s. The 3×10^{-15} frequency stability specification is almost met for $\tau \leq 1,000$ s limited by a flycker floor [14] (cf. Fig. 7). This result corresponds to a data recording of about 5 hours (15192 samples) without any post-processing applied to the raw data. The resulting beatnote signal was compared to the output of a RF synthesizer HP8662A. The CSO's phase noise has been measured by demodulating the 745kHz beatnote with the signal coming from a divided RF synthesizer [15]

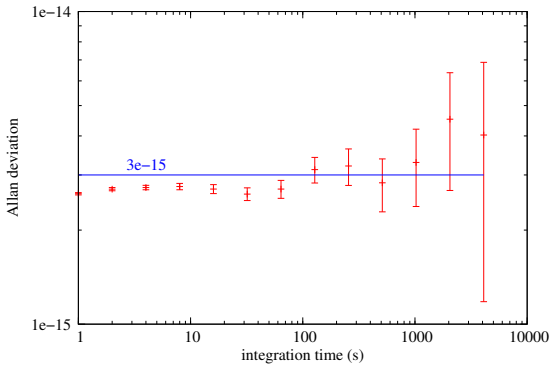

Figure 7: *Maximal frequency instability of the cryocooled CSO Elisa measured by direct comparison with Alizée cooled in a liquid helium bath.*

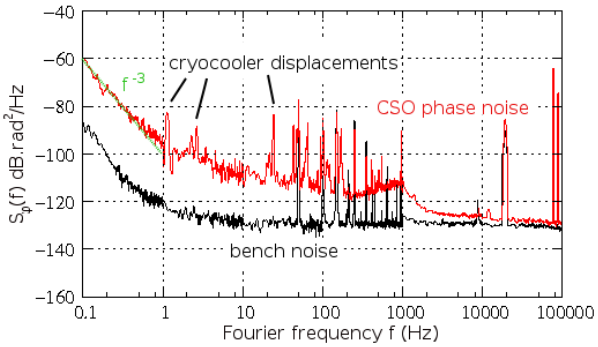

Figure 8: *Phase noise of Elisa.*

At low Fourier frequencies, the measured phase noise is dominated by a flicker frequency noise (f^{-3} slope). For one CSO, we get $S_\phi(1Hz) = -98$ dB.rad^2/Hz equivalent at $\sigma_y(1s) \approx 1.5 \times 10^{-15}$ in the time domain. This result is coherent

with the $\sigma_y(1s) \approx 2.6 \times 10^{-15}/\sqrt{2} \approx 1.8 \times 10^{-15}$ measured previously. On the same spectrum, bright lines resulting from the residual vibrations are clearly visible. from the power of first line at 1.14 Hz, we estimated that the residual displacement of the resonator is less than 1 μm.

8.2 Latest results

A new tuning of the servo controls improved the short term frequency stability of Elisa and Alizée as indicated in red in Fig. 9. The flicker floor decreased until 1.5×10^{-15} reached at 20s. At longer integration time, the CSOs are limited by a random walk $\sigma_y(\tau) \approx 1.3 \times 10^{-16}\sqrt{\tau}$. The figure 10 shows a strong dependence between the atmospheric pressure fluctuations and the beatnote frequency variations. It means that the output signal frequency of one or each CSO is strongly sensitive to the pressure fluctuations. We estimated a sensitivity about:

$$\frac{1}{P_{atm}}\frac{\delta\nu}{\nu_0} \approx 7.2 \times 10^{-14}/mbar \quad (1)$$

If we assumed a daily atmospheric pressure variation around 5 mbars, the frequency stability of the beatnote signal is limited at $\approx 3 \times 10^{-13}$/day which explains the observed stability limitation at long integration times. We are confident that this pressure sensitivity is only due to Alizée which is cooled down in the liquid helium bath. Indeed, the liquid helium evaporation temperature is strongly dependent on the pressure (≈ 1 mK/mbar).

In the same conditions, we measured the frequency stability of the operational outputs of the frequency synthesis. The frequency of the DDS of one of the synthesis was shifted to produce a beatnote signal between each CSO's synthesis. The frequency instabilities of the resulting signal were measured with the use of high resolution counter. The Allan deviation of the 10GHz and 100MHz operational frequencies are indicated respectively in black and green in Fig. 9.

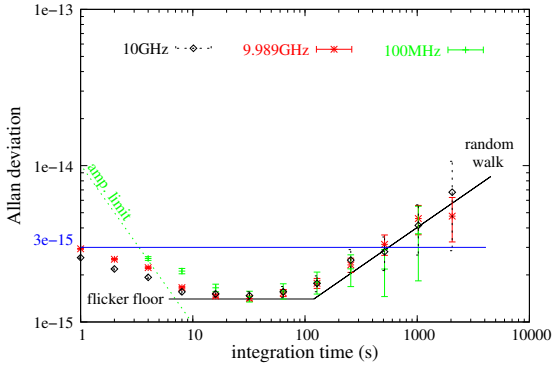

Figure 9: *Allan deviation of the resulting beatnote signals at 10GHz (black curve), 9.989GHz (red curve) and 100MHz (green curve).*

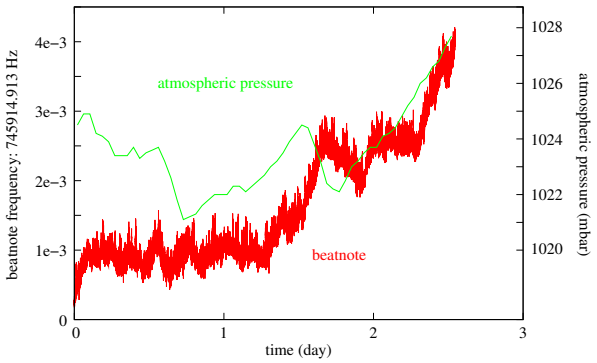

Figure 10: *Atmospheric pressure fluctions against beatnote frequency variations.*

The frequency synthesis enables to transfer the CSO performances at the operational frequencies of 10GHz and 100MHz.

9 CONCLUSION

This article sumarizes the latest results obtained on the Elisa project founded by the European Space agency. This study led to the development of a cryocooled sapphire oscillator named Elisa. Elisa shows an exceptional Allan deviation inferior of 3×10^{-15} for integration times ranging from 1s to 1000s for a phase noise of $S_\phi(1Hz) = -98$ dB.rad^2. Moreover, the frequency synthesis enables to transfer the performances of Elisa at the operational frequencies of 10GHz and 100MHz.

References

[1] http://www.crystalsystem/.

[2] http://www.amlj.com/lowphasenoise.html/.

[3] E. BLACK : An introduction to Pound-Drever-Hall laser frequency stabilization. Am. J. Phys, 1:79–87, jan. 2001.

[4] S. CAPARELLI, E. MAJORANA, V. MOSCATELLI, E. PASCUCCI, M. PERCIBALLI, P. PUPPO, P. RAPAGNANI et F. RICCI : Vibration-free cryostat for low-noise applications of a pulse tube cryocooler. Review of Scientific Instruments, 77:095102–1–7, 2006.

[5] S. CHANG et A. MANN : Mechanical stress caused frequency drift in cryogenic sapphire resonator. In Proc. of the 2001 IEEE International Frequency Control Symposium, p. 710–714, Seattle, WA, USA, june 6-8 2001.

[6] W. DAL, E. GMELIN et R. KREMER : Magnetothermal properties of sintered $Gd_3Ga_5O_{12}$. J. Phys. D: Appl. Phys, 21:628–635, 1988.

[7] R. DREVER, J. HALL, F. KOWALSKI, J. HOUGH, G. FORD, A. MUNLEY et H. WARD : Laser phase and frequency stabilization using an optical resonator. Appl. Phys. B, 31:97–105, 1983.

[8] Z. GALANI, M. BIANCHINI, W. JR., C. RAYMOND, R. DIBIASE, R. LATON et J. BRADFORD COLE : Analysis and design of a single-resonator gaas fet oscillator with noise gegeneration. IEEE Transactions on Microwave Theory and Techniques, 32(12):1556–1565, december 1984.

[9] S. GROP, P. BOURGEOIS, N. BAZIN, C. LANGHAM, M. OXBORROW, J. D. V. E. RUBIOLA, Y. KERSALÉ et V. GIORDANO : ELISA : An ultra-stable oscillator for esa deep space antennas. In Proc. of the joint meeting IFCS-EFTF, p. 376–380, Besançon, France, april 20-24 2009.

[10] S. GROP, V. GIORDANO, P. BOURGEOIS, Y. KERSALÉ, N. BAZIN, M. OXBORROW, G. MARRA, C. LANGHAM, E. RUBIOLA et J. DE VICENTE : ELISA: an ultra-stable frequency reference for space mission ground segment. In Microwave Technology and Techniques Workshop 2008 - Innovations and Challenges., p. 06_Grop, ESA/ESTEC Noordwijk, The Nederlands, 6-7 May 2008.

[11] J. KRUPKA, D. CROS, A. LUITEN et M. TOBAR : Design of very high q sapphire resonators. Electronics Letters, 32:670–671, 1996.

[12] C. R. LOCKE, E. N. IVANOV, J. G. HARTNETT, P. L. STANWIX et M. E. TOBAR : Design techniques and noise properties of ultrastable cryogenically cooled sapphire-dielectric resonator oscillators. Review of Scientific Instruments, 79:051301–1–12, 2008.

[13] E. RUBIOLA : Phase noise and frequency stability in oscillators. Cambridge University Press, 2008. ISBN 978-0-521-88677-2.

[14] N. B. Y. K. E. R. C. L. M. O. D. C. S. W. J. D. V. S. GROP, P.Y. Bourgeois et V. GIORDANO : Elisa: a cryocooled 10 ghz oscillator with 10^{-15} frequency stability. Review of Scientific Instruments, 81:81, 1–1, 2010.

[15] R. B. Y. K. E. R. S. GROP, P.Y. Bourgeois et V. GIORDANO : 10 ghz cryocooled sapphire oscillator with extremely low phase noise. Electronics Letters.

[16] T. TOMARU, T. SUZUKI, T. HARUYAMA, T. SHINTOMI, N. SATO, A. YAMAMOTO, Y. IKUSHIMA, R. LI, T. AKUTSU, T. UCHIYAMA et S. MIYOKI : Cryocoolers 13, chap. Vibration-Free Pulse Tube Cryocooler System for Gravitational Wave Detectors, Part I: Vibration-Reduction Method and Measurement, p. 695–702. Springer US, 2005.